Thermochimica Acta, 88 (1985) 443–451
Elsevier Science Publishers B.V., Amsterdam – Printed in The Netherlands

THERMAL STUDIES ON SODIUM SILICATE HYDRATES. IV. THERMAL STABILITY OF SODIUM SILICATE HYDRATES $Na_2[SiO_2(OH)_2]\cdot nH_2O$ ($n = 4, 5, 7, 8$). PHASE RELATIONS AND DECOMPOSITION CHARACTERISTICS UNDER OPEN-SYSTEM CONDITIONS

J. FELSCHE, B. KETTERER and R.L. SCHMID

Fakultät für Chemie, Universität Konstanz, Postfach 5560, D-7750 Konstanz (F.R.G.)

(Received 27 December 1984)

ABSTRACT

Thermoanalytic studies carried out on hydrate phases $Na_2[SiO_2(OH)_2]\cdot nH_2O$ ($n = 4$, 5, 7, 8) reveal two phase transitions at elevated temperatures under open-system and non-isothermal conditions

$$Na_2[SiO_2(OH)_2]\cdot nH_2O(s) \xrightarrow{T_{mp}} Na_2[SiO_2(OH)_2]\cdot nH_2O(l)$$

$$Na_2[SiO_2(OH)_2]\cdot nH_2O(l) \xrightarrow{T_c} Na_2[SiO_3](s) + (n+1)H_2O(g)$$

Congruent melting at temperatures T_{mp} is followed by condensation at temperatures $T_c >$ 380 K with subsequent formation of solid $Na_2[SiO_3]$. Foaming of the melts upon condensation is observed through heating stage microscopy. In situ ^{29}Si NMR experiments proved oligomeric or endless chain-type anions, $[Si_{1+n}O_{2+3n}(OH)_2]^{(2+2n)-}$, to be formed in the melts under open-system conditions. From DTA double peak configurations at temperatures T_c the thermal decomposition of the melts is shown to occur in a two-step reaction, uniformly with all four hydrate phases.

Isothermal studies below melting temperatures show distinct decomposition of crystalline $Na_2[SiO_2(OH)_2]\cdot 8H_2O$ to crystalline $Na_2[SiO_2(OH)_2]\cdot 4H_2O$, whereas all the other crystalline phases within this hydrate series dehydrate to amorphous waterglass-type materials under identical experimental conditions in long-term annealing experiments. This exceptional phase relation between the octa- and the tetrahydrate has also been proved by X-ray powder diffraction heating experiments.

INTRODUCTION

Within a general revision of the system Na_2O–SiO_2–H_2O, which is especially concerned with structure-to-thermal-property relationships of sodium silicate hydrate phases, we have so far reported on the decomposition characteristics, phase relations and structures of the hydrates $Na_3[SiO_3(OH)]\cdot nH_2O$ ($n = 5$, 2, 1, 0) [1–4]. Hydrates of the series

0040-6031/85/$03.30

$Na_2[SiO_2(OH)_2]\cdot nH_2O$ ($n = 4, 5, 7, 8$) are of special interest because of their congruent melting behavior and special features of supercooled melts. Neutron diffraction data on crystal structures of the disodium dihydroxysilicate hydrates [6–8] have been accomplished in order to achieve a better understanding of the distinct thermodynamic properties from special features in hydrogen bonding. We will extend the previously given data on thermal properties [5], which were from DSC experiments under closed-system conditions essentially, to thermal decomposition characteristics under open-system conditions, here. Special thermodynamic properties, such as P_{H_2O} partial pressure data as a reply on corresponding experiments described by Gould et al. [9,10], will be discussed in a forthcoming paper.

EXPERIMENTAL

Pure-phase single crystals of all four hydrates $Na_2[SiO_2(OH)_2]\cdot nH_2O$ ($n = 4, 5, 7, 8$) have been grown by different approaches of various crystal growth techniques in order to meet the demands for unambiguous results from thermoanalysis and heating microscopy. Smaller fractions or twinned materials have been supplied for the corresponding samples for X-ray powder diffraction work.

Employing high-grade Na_2CO_3 (Merck 6392E) and $SiO_2\cdot nH_2O$ (Merck 657) as starting materials, pure-phase metasilicate Na_2SiO_3 was obtained through the following sequence of reactions.

$$Na_2CO_3 + SiO_2 \xrightarrow[\text{calcination}]{\text{973 K, 24 h}} Na_2SiO_3 + CO_2 \xrightarrow[\text{melting}]{\text{1361 K, 1h}} Na_2SiO_3$$

$$Na_2SiO_3\ (\text{glass}) \xrightarrow[\text{recrystallization}]{\text{973 K, 24 h}} Na_2SiO_3\ (\text{cryst.})$$

Compact samples of polycrystalline metasilicate were ground to 25–50 μm·particle size for subsequent hydrolysis at elevated temperatures under CO_2-free but open-system conditions (Braun glovebox MB 200). Single crystals of the octahydrate, up to 20 mm size, have been grown from nearly stoichiometric solutions (6.5% Na_2O/6.2% SiO_2/87.3% H_2O) and those of the tetrahydrate with considerable excess of NaOH (45% Na_2O/10% SiO_2/45% H_2O) at temperatures of 298 K after addition of a small fraction of seed crystals from selected samples of pure-phase material. Crystals of $Na_2[SiO_2(OH)_2]\cdot 5H_2O$ have been obtained from solutions of 20.5% Na_2O/9.8% SiO_2/69.7% H_2O at 291 K and those of $Na_2[SiO_2(OH)_2]\cdot 7H_2O$ from 11.19% Na_2O/11.53% SiO_2/76.92% H_2O at temperatures of 298 K under CO_2-free atmosphere. (All concentrations are given in wt.%.)

The constitution of polycrystalline or single crystal phases has been proved by Guinier X-ray diffraction or precession techniques and polarization microscopy.

The thermoanalytical experiments have been carried out on a Netzsch STA-429 thermoanalyzer (TG, DTG and DTA) under pure and dry N_2 atmosphere employing simultaneous mass spectrometry (Balzers QMG 511) in order to specify gaseous decomposition products. The leak system to our mass spectrometer is similar to that previously described by Eppler and Selhofer [11] and Yoen et al. [12].

For X-ray diffraction studies a Guinier heating camera with gasflow heating device (296–1200 K) and a Guinier film camera (System 621, Huber, Rimsting, $\lambda Cu K\alpha_1$) have been employed. Corresponding heating microscopy has been carried out on a Wild M400 photomacroscope employing a heating stage equipment (Leitz, Wetzlar).

The ^{29}Si NMR experiments have been carried out on a Bruker CXP 300 instrument. MAS (magic angle spinning) frequencies of 400–3200 Hertz and a gas flow heating equipment allowed for temperature-controlled runs (150–450 K) on polycrystalline samples (30–50 μm).

RESULTS AND DISCUSSION

Thermal properties of sodium silicate hydrates $Na_2[SiO_2(OH)_2]\cdot nH_2O$ ($n = 4, 5, 7, 8$) have been studied under non-isothermal and isothermal open-system conditions (dry nitrogen atmosphere, normal pressure) at temperatures up to 1000 K.

Figure 1 gives the corresponding thermogravimetric (TG) and DTA data from non-isothermal runs with heating rates of 5 K min^{-1}. TG curves show the thermal stability of all the given hydrate phases up to melting and subsequent decomposition yielding metasilicate, Na_2SiO_3, which has been proved to be crystalline at temperatures, $T > 450$ K from Guinier powder diffraction data. DTA curves show endothermic peaks at temperatures of 325, 326, 345 and 352 K from congruent melting of the tetra-, penta-, hepta- and octahydrate, respectively. Melting temperatures are slightly increased as compared to DSC data from closed-system conditions [5]. Evaporation of H_2O, which starts upon melting, is rapidly increased with increasing temperature. From the characteristic double peaks at temperatures of 380–420 K a two-step decomposition reaction of melts is indicated for all four hydrate phases uniformly.

Heating stage microscopy (Fig. 2) shows capsulation of the melt of an $Na_2[SiO_2(OH)_2]\cdot 8H_2O$ crystal at 375 K produced by dehydration of the sample surface

$$Na(OH_2)_n \overset{T > T_{mp}}{\rightarrow} Na(OH_2)_{n-x} + xH_2O$$

Subsequent boiling bubbles occurring and increase of sample volume finally yields a solid and opaque foam at temperatures, $T > 450$ K, which consists

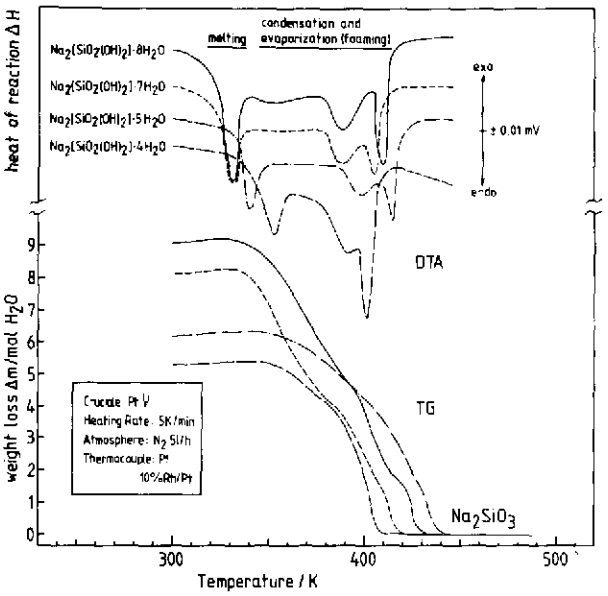

Fig. 1. Thermograms of the thermal decomposition of single crystals (1–2 mm in diameter) of $Na_2[SiO_2(OH)_2]\cdot nH_2O$ ($n = 8, 7, 5, 4$) under non-isothermal and open-system conditions. TG and DTA curves show decomposition of individual phases starting immediately after congruent melting. Melting temperatures, here from samples under dry nitrogen atmosphere, are slightly increased as compared to closed-system conditions [5]. Two further peaks closely related to each other occur at elevated temperatures (380–420 K). Those endothermic double peaks verify the complex nature of decomposition of the homogeneous melts. Dehydratation and dehydroxylation of $[Na(OH_2)_n]^+$ or $[SiO_2(OH)_2]^{2-}$ groupings, respectively, suffer from capsulation of the sample by waterglass-type material $Na_2SiO_3\cdot xH_2O$ with $x < n$. Further H_2O molecules accumulate from proceeding condensation inside the sample. Because of the increasing partial pressure of gaseous H_2O, bubbles show up inside the melts (see Fig. 2/375 K). Bubbles grow with subsequent extension of the sample's overall volume. We observe foaming of the sample through this period of the reaction from heating stage microscopy (Fig. 2). TG curves show discontinuities in slopes at corresponding temperatures, which means that the release of water molecules from the sample is hindered at temperatures which correlate to the first DTA peaks (period of capsulation) but breaks through at slightly elevated temperatures, which agrees with the second DTA peak of double peak configuration. The final decomposition product of all four hydrate phases shown is polycrystalline Na_2SiO_3 from Guinier X-ray diffraction data on the given samples or from corresponding X-ray heating experiments (compare fig. 6 or fig. 3 in ref. 7).

amorphous or polycrystalline Na_2SiO_3, prevailingly. DTA double peaks at temperatures of 380–420 K (Fig. 1) which correspond to the visible features of sample capsulation and subsequent foaming, might be understood in terms of two different but correlated reactions. The starting reaction, which is of chemical nature, is given by condensation of monomeric-type silicate anions

$$[SiO_2(OH)_2]^{2-} + n[SiO_2(OH)_2]^{2-} \xrightarrow{380\text{–}400\ K} [Si_{1+n}O_{2+3n}(OH)_2]^{(2+2n)-} + nH_2O$$

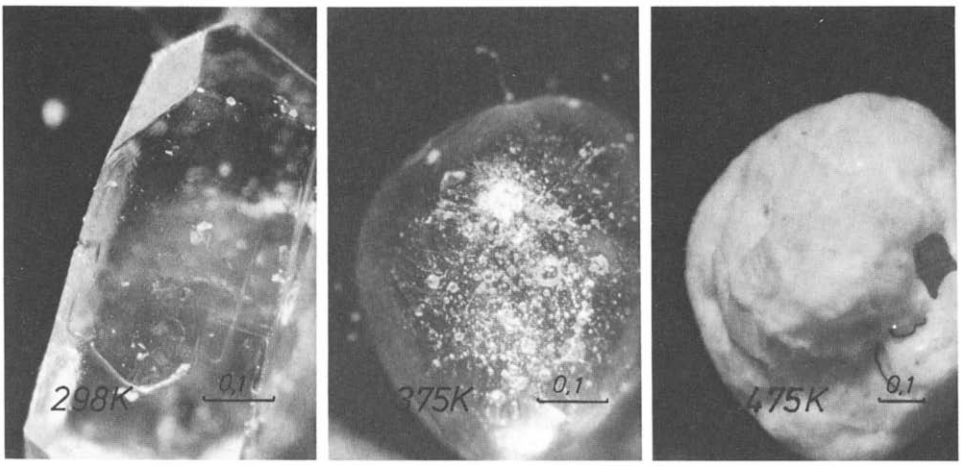

Fig. 2. Thermal decomposition of $Na_2[SiO_2(OH)_2]\cdot 8H_2O$ as observed by heating stage microscopy. The photographs (from the left) show three stages of the material: single crystal at room temperature (298 K), spherical melt in the period of starting decomposition at 375 K and, finally, the polycrystalline decomposition product at 475 K. Note that the scale given in length of 0.1 mm is reduced in the photograph at 475 K (right). This means that the compact sphere of the melt shown at 375 K, extends in volume hy a factor of about 10 in the course of the subsequent decomposition reaction. Thermal decomposition of the melt, which correlates the DTA double peak at 390/410 K in Fig. 1, shows up with foaming of the sample. Gaseous H_2O from dehydration and condensation serves as the propellent agent in the foaming process which finally yields dry polycrystalline Na_2SiO_3 material at elevated temperatures (compare fig. 6 or fig. 3 in ref. 5).

$$[Si_{1+n}O_{2+3n}(OH)_2]^{(2+2n)-} + nH_2O(g) \xrightarrow{400\text{–}420\ K} [SiO_3]_{1d\infty} + H_2O(g)$$

to chain-like silicate oligomers and to the endless chain anion $[SiO_3]^{2-}$, finally.

^{29}Si NMR in situ heating experiments confirm some further details of this reaction (Fig. 3). The MAS data on $[Na_2SiO_2(OH)_2]\cdot 4H_2O$ at 345 K (crystal) and 370 K (melt) show that the essential structural features around the monomer anion $[SiO_2(OH)_2]^{2-}$ remain unchanged through the phase transition of congruent melting at 365 K. Condensation products of oligomer-type silicate anions $[Si_{1+n}O_{2+3n}(OH)_2]^{(2+2n)-}$ predominantly occur at elevated temperatures of 393 and 423 K. Because of limitation in the gas stream heating equipment in situ ^{29}Si NMR experiments have not been extended to higher temperatures. From Guinier powder diffraction work we know, however, that the formation of polymeric anions $[SiO_3]^{2-}_{1d\infty}$ is rapidly increased at temperatures, $T > 420$ K (compare fig. 3 in ref. 5).

The process of condensation is obviously hindered by capsulation of the samples, which suppresses further escape of water molecules from the water-glass-like materials. Discontinuities in the TG curves (Fig. 1) verify this interruption in overall decomposition. DTA curves also show intersec-

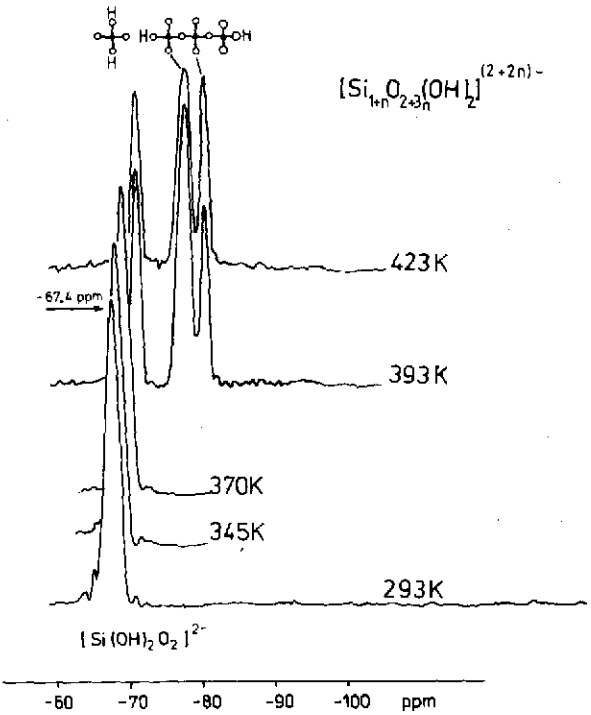

Fig. 3. ^{29}Si NMR spectra of $Na_2[SiO_2(OH)_2]\cdot 4H_2O$ at temperatures of 293, 345, 370, 393 and 423 K (gas flow heating equipment). Magic angle spinning (MAS) frequencies of 3200 Hz for 293 and 345 K experiments, 400 Hz at elevated temperatures of 370 K, 393 and 423 K, employing TMS and Q_8M_8 standards (Bruker CXP 300). The spectra confirm the isostructural relationship between crystal (293, 345 K) and melt (370 K), the 370 K spectrum taken immediately beyond the melting temperature of 365 K. The −67.4 ppm chemical shift peak of the monomeric tetrahedral silicate anion $[SiO_2(OH)_2]^{2-}$ shows a slight high field shift for 293–393 K spectra. Oligomer-type hydroxy-silicate anions $[Si_{1+n}O_{2+3n}(OH)_2]^{(2+2n)-}$ or the endless chain-type anion $[SiO_3]^{2-}_{1d\infty}$ occur at elevated temperatures of 393 and 423 K, when condensation proceeds.

tions in their endothermic peak characteristics. From heating stage microscopy we see that the volume of the sample considerably increases during this period of the reaction. Gaseous H_2O, enriched inside the sample, extends bubbles in the melts thus serving as a propellent agent in the foaming process. From the microscopic study we suggested that the foaming is completed in time with the occurrence of the second peak in the endothermic DTA double peak characteristics. The stronger second DTA peak is from the prevailing evaporation enthalpy of H_2O, which is released from the porous material as soon as the thin waterglass walls crash by the elevated H_2O pressure inside the bubbles. Thus, the latter part of the decomposition of the melts is essentially of physical nature. The increasing viscosity of the melt occurring simultaneously with the loss of water is another essential feature of this decomposition reaction. The overall reaction is strongly

controlled by kinetics. Single crystals or polycrystalline samples of different grain size show significant deviations in their DTA double peak profile due to individual heating rates, atmospheres and various effects from transport and surface properties.

Further details on the foaming process and physical data on waterglass-type foams will be discussed elsewhere.

In Fig. 4 the hypothetical T,x phase diagram of the system Na_2SiO_3–H_2O within the region of molar compositions 80–91% H_2O at temperatures 273–484 K is shown. Data from non-isothermal runs under closed-system conditions [5], e.g., melting point temperatures, or from open-system conditions from this study are summarized.

Isothermal studies on the thermal stability of the given series of disodium dihydrogensilicate hydrates (Fig. 5) showed an exceptional relation between the octa- and tetrahydrate under open-system conditions (dry nitrogen atmosphere (99.999%), normal pressure)

$$Na_2[SiO_2(OH)_2]\cdot 8H_2O \xrightarrow[N_2,\ 760\ Torr]{T<T_{mp}} Na_2[SiO_2(OH)_2]\cdot 4H_2O + 4H_2O(g)$$

Long-term annealing experiments at temperatures below the melting point (T_{mp} – 325 K) revealed the tetrahydrated phase to be the only crystalline decomposition product. No contributions of the hepta- or pentahydrate have ever been observed in decomposition products of the octahydrate. On the other hand, the hepta- and pentahydrate never show the tetrahydrate or any

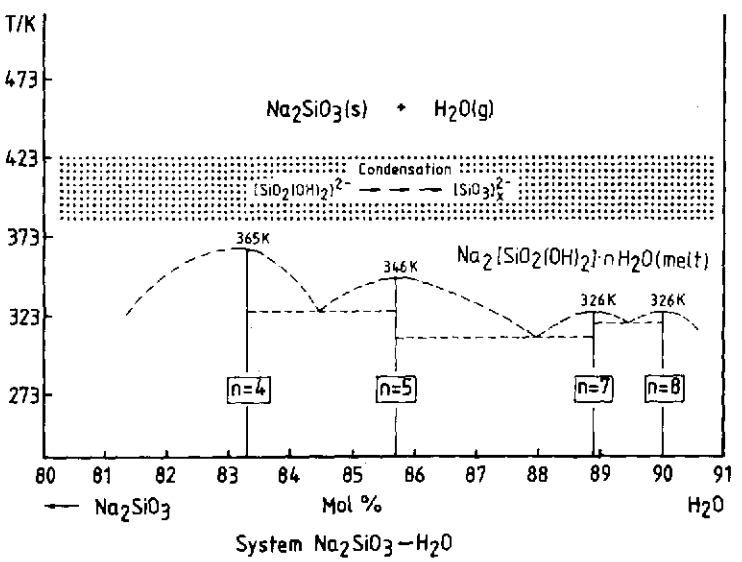

Fig. 4. T,x phase diagram of the system Na_2SiO_3–H_2O at molar compositions 80–91% H_2O and temperatures 273–473 K. Congruent melting characteristics of compounds $Na_2[SiO_2OH)_2]\cdot nH_2O$ (n = 4, 5, 7, 8) are from closed-system conditions [5].

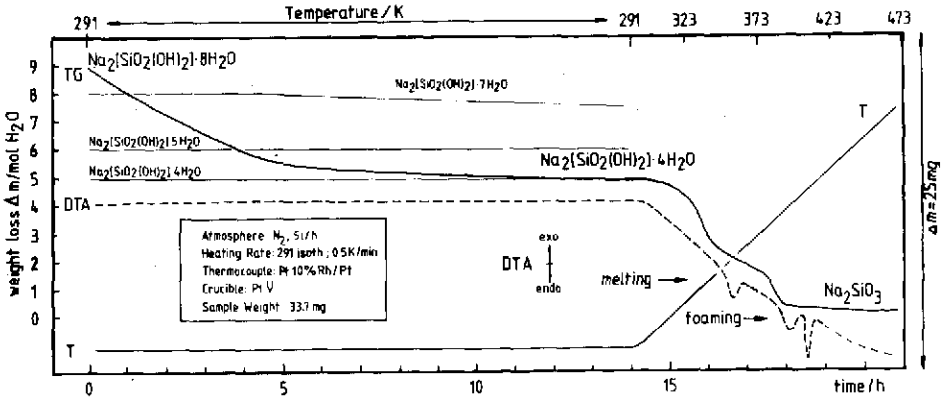

Fig. 5. Thermal decomposition characteristics of compounds $Na_2[SiO_2(OH)_2]\cdot nH_2O$ (single crystals, 1–2 mm in diameter) under isothermal (291 K) and open-system conditions (dry nitrogen atmosphere). The octahydrate decomposes into the crystalline phase of the tetrahydrate within 10 h, whereas all the other hydrate phases show fairly low decomposition rates but amorphous contributions from decomposition. The tetrahydrate reveals the most outstanding thermal stability. Subsequent heating of the decomposition product $Na_2[SiO_2(OH)_2]\cdot 4H_2O$ yields the well-known melting and decomposition characteristics (compare Fig. 1).

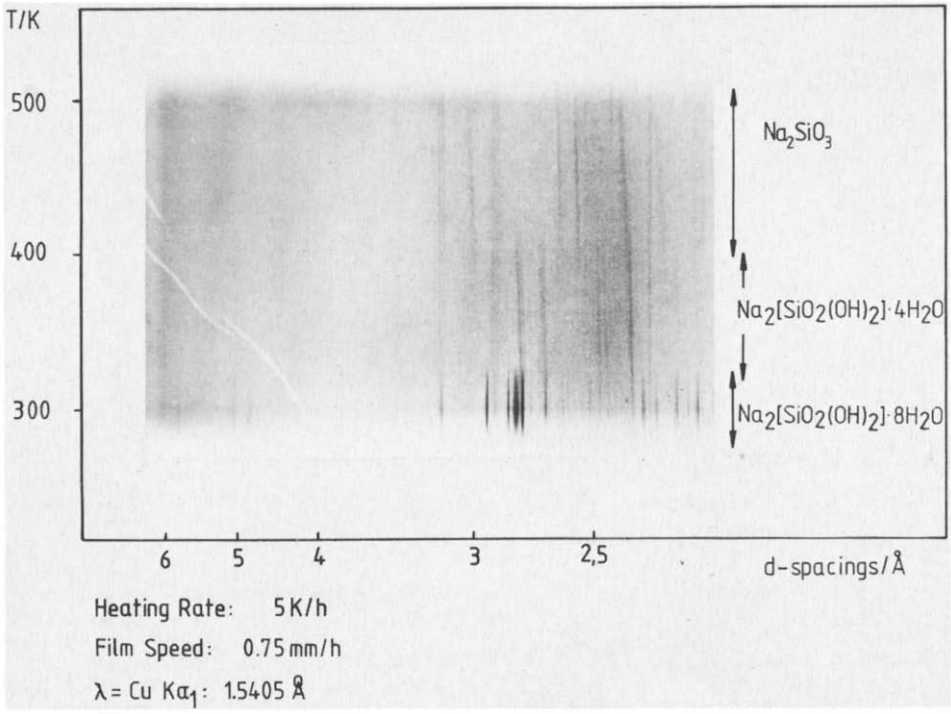

Fig. 6. X-ray heating photograph of $Na_2[SiO_2(OH)]\cdot 8H_2O$. (Guinier camera; Cu $K\alpha_1$ radiation; heating rate, 5 K h^{-1}; film speed, 0.75 mm h^{-1}; quartz glass tube, 0.5 mm; open-system conditions). The polycrystalline sample of the octahydrate decomposes to the corresponding tetrahydrate at rather low temperatures of about 320 K. At elevated temperatures ($T > 400$ K) the diffraction pattern of metasilicate Na_2SiO_3 shows up.

other subhydrate phase from decomposition, but essentially amorphous waterglass-like phases.

The exceptional relationship between the octa- and tetrahydrate also shows up in X-ray diffraction heating photographs carried out at a heating rate of 5 K h^{-1}. The Guinier photograph of Fig. 6 shows the tetrahydrate immediatedly following the octahydrate at temperatures of about 325 K, whereas any other hydrate phase of this sodium silicate series yields an amorphous phase upon melting under identical experimental conditions (compare fig. 3 in ref. 5). The final decomposition products, however, proved to be crystalline Na_2SiO_3 for all the given hydrates.

Re-hydration of partly or completely dehydrated samples failed under any experimental conditions, employing various H_2O partial pressures under isothermal temperatures $T < T_{mp}$. Hydrolysis has been observed in all the long-term annealing experiments at 100% relative humidity, yielding heterogeneous liquids or solids. The tetrahydrate showed up with a considerable long-term stability in humid, regular or dry atmospheres as compared to any other hydrate phases within this sodium silicate hydrate series.

ACKNOWLEDGEMENTS

The Deutsche Forschungsgemeinschaft, Bonn-Bad Godesberg is gratefully acknowledged for financial support. The authors are indebted to Dr. Förster, Bruker GmbH, Karlsruhe, who carried out some of the NMR experiments and to G. Wildermuth and A. Straub for technical assistance.

REFERENCES

1 R.L. Schmid and J. Felsche, Thermochim. Acta, 71 (1983) 359.
2 R.L. Schmid and J. Felsche, Thermochim. Acta, 79 (1984) 243.
3 R.L. Schmid, G. Huttner and J. Flesche, Acta Crystallogr., Sect. B, 35 (1979) 3024.
4 R.L. Schmid, G. Huttner, L. Szolnay and J. Felsche, Acta Crystallogr., Sect. B, 37 (1981) 789.
5 J. Felsche, B. Ketterer and R.L. Schmid, Thermochim. Acta, 77 (1984) 109.
6 L.S. Dent-Glasser and P.B. Jamieson, Acta Crystallogr., Sect. B, 32 (1976) 705.
7 R.L. Schmid, J. Felsche and G.J. McIntyre, Acta Crystallogr., Sect. C, 40 (1984) 733.
8 R.L. Schmid, J. Felsche and G.J. McIntyre, Acta Crystallogr., Sect. C, 41 (1985) in press.
9 R.O. Gould, B.M. Lowe and McGilp, Thermochim. Acta, 14 (1976) 299.
10 R.O. Gould, B.M. Lowe and McGilp, J. Chem. Thermodyn., 8 (1976) 277.
11 H. Eppler and H. Selhofer, Thermochim. Acta, 20 (1977) 45.
12 H.K. Yuen, G.W. Mappes and W.A. Grotz, Thermochim. Acta, 52 (1982) 143.